PERGAMON

Materials Science in Semiconductor Processing 3 (2000) 227–235

MATERIALS SCIENCE IN SEMICONDUCTOR PROCESSING

Intrinsic defects in silicon

George D. Watkins*

Department of Physics, Lehigh University, 16 Memorial Dr. East, Bethlehem, PA 18015, USA

Abstract

A review is given of what has been learned from electron paramagnetic resonance (EPR) and localized vibrational mode (LVM) spectroscopy concerning isolated lattice vacancies and self-interstitials, and their interactions with other defects in silicon. This information can supply the basic tools with which to help unravel much of the complex processes and structures involved in crystal growth, device processing, and radiation damage.

Keywords: Silicon; Vacancy; Self-interstitial; Migration; Diffusion

1. Introduction

Understanding the intrinsic defects in silicon — lattice vacancies and interstitials — represents the first logical step toward unraveling radiation damage in the material, because these are the primary defects produced as incoming particles collide with and displace the host atoms. It is also the first logical step toward unraveling the structure and properties of the many complex grown-in and process-induced defects involved in silicon technology. They are obviously the fundamental building blocks for vacancy and interstitial aggregates, voids, interstitial loops, etc. But even dislocations, grain boundaries, interfaces, and external surfaces can be considered to be various geometric arrays of these fundamental point defects. And these complex defects can act, in turn, as sinks and/or sources for vacancies and interstitials following a radiation damage event and/or during the various processing steps in device preparation.

In the present paper I will review therefore what has been learned about these intrinsic defects[1] over the past ~40 years [1–5].[2,3] As I will demonstrate, a great deal has indeed been learned about them and their interactions with other defects.

2. Production of vacancies and interstitials

The first required step in unraveling the properties of the defects is to produce *isolated* single vacancies and interstitials for study. The only procedure that has been found to work is ~1–3 MeV electron irradiation performed at cryogenic temperatures. In so doing, the atoms are displaced by Rutherford scattering of the high-energy electron, the low mass of the electron assuring simple damage since the recoiling nucleus obtains little excess kinetic energy, discouraging further atomic displacements by it. The cryogenic temperature is required to freeze in the displacement products. The

*Corresponding author. Tel.: +1-610-758-3961; fax: +1-610-758-4561.

E-mail address: gdw0@lehigh.edu (G.D. Watkins).

[1] For a more complete description of the properties to be described here of the vacancies and interstitials and their interactions with other defects, with proper references to the literature, see references [1,2] and [3], below. No attempt will be made therefore to supply detailed literature references here, except as needed to supplement those contained therein. The present review follows closely the outline of similar reviews given by the author (e.g., Ref. [4] below), but it has been brought up to date to include important recent results.

[2] A substantially revised and updated revision of Ref. [1] is now available in [2].

[3] Ref. [3] deals with the vacancy only, but in greater detail.

1369-8001/00/$ - see front matter
PII: S1369-8001(00)00037-8

additional advantage of electron irradiation is that an electron is not an impurity and only displacement of the host atoms can result.

The scenario expected for such an experiment is as follows: Interstitials and vacancies will be formed by pairs as lattice atoms are displaced by the incoming electrons. As the temperature is raised, either interstitials or vacancies will become mobile first, some recombining with their partners, the others diffusing away through the lattice to become trapped by other impurities or defects. At a still higher temperature the other partner will become mobile and will diffuse through the lattice until trapped.

In what follows, I will concentrate primarily on the results of such studies using electron paramagnetic resonance (EPR) spectroscopy performed in situ in the irradiation apparatus. With EPR it has been possible to *identify* the defects, their chemical constituents, their atomic lattice structures, and to follow and identify their various reactions as they begin to migrate and interact with other defects. EPR provides this unique information because of the resolved anisotropy and near-neighbor hyperfine interactions that its spectra often contain. Recently, local vibrational mode (LVM) spectroscopy has also been demonstrated to provide reliable defect information in some cases for intrinsic defects trapped by light atom impurities. I will also include this information where appropriate. Here, isotope shifts, and symmetry determination from shifts and alignments under applied uniaxial stress, supply the identifying features. Once identified by these techniques, the information obtained by correlated electrical measurements and optical spectroscopy has also contributed significantly to our understanding, and some of this will also be briefly described.

3. The lattice vacancy

The isolated lattice vacancy has been observed by EPR in its single positive (V^+) and negative (V^-) charge states immediately after in situ electron irradiation at 4.2 K. The primary identification feature in these cases is the detection of hyperfine interaction with the 4.7% abundant magnetically active ^{29}Si atom nucleus located at each of the four atom sites surrounding the vacancy. By monitoring the spectra of these two charge states vs. Fermi level, optical excitation, applied uniaxial stress, etc., it has been established that the vacancy actually takes on five different charge states in the silicon band gap (V^{2+}, V^+, V^0, V^-, V^{2-}). This is summarized in Fig. 1, which shows also the lattice relaxations deduced for four of them that occur as the broken bonds reconstruct in different ways vs. charge state.

These reconstructions are very important: (1) They become increasingly strong as the defect picks up

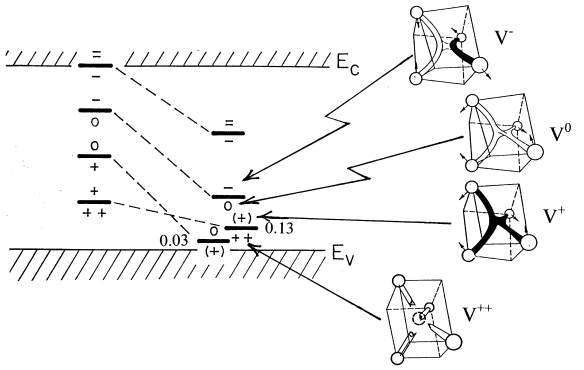

Fig. 1. Level positions for the lattice vacancy, before, and after, lattice relaxations, as shown in the insets. The darkened bonds indicate the location of the electronic spin seen in the EPR.

electrons, which serves to crowd more available charge states into the gap. This is illustrated in the figure by first illustrating the uniform level separation expected before distortion (Coulomb repulsion energy for each added electron), and then their lowering due to the energy gain by the distortions. The positions of two of the levels have been firmly established, shown in eV above the valence band edge, which reveals another remarkable effect. Their level ordering is reversed, a phenomenon known as "negative-U", where the second electron is bound more strongly to the V^{2+} core than the first. This phenomenon, a direct result in this case of the large lattice relaxation, the energy gain from which exceeds the Coulomb repulsion energy, is of great current interest in the scientific community. The isolated vacancy is one of the first such defects to be discovered, and has served as a model for the understanding of the phenomenon.[4] (2) The existence of many charge states and their differing lattice reconstructions means that the diffusion properties of the vacancy and its subsequent interactions with other charged defects can also be expected to depend upon its charge state. (3) Capture of carriers at the defect can serve to dump vibrational energy into the defect as the atoms are propelled toward their configurations in the new charge state, and, as we shall demonstrate, this will serve, in turn to assist its migration, a phenomenon known as "recombination-enhanced migration" (REM) [7–9].

4. Vacancy diffusion

The vacancy spectra disappear in a 15 min isochronal annealing sequence at ~70 K in n-type, ~150 K in

[4] For a detailed description of the experiments establishing the negative-U properties of the vacancy (and interstitial boron), in addition to a general discussion of the phenomenon, see [6].

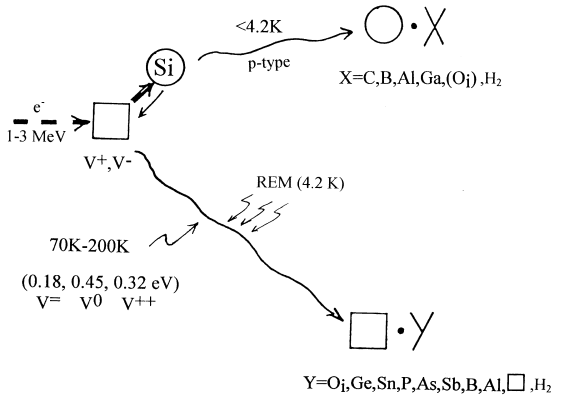

Fig. 2. Summary of vacancy and interstitial reactions after 4.2 K e-irradiation.

p-type, and ~200 K in high-resistivity material. The simultaneous growth of new spectra that have been identified as vacancies paired off with other defects establishes unambiguously that the process is a long-range diffusion of the vacancy. This is summarized in Fig. 2, where vacancies trapped by interstitial oxygen, isoelectronic substitutional impurities (Ge, Sn), substitutional donors (P, As, Sb), substitutional acceptors (B, Al), and other vacancies to produce divacancies, have all been identified, and observed to emerge in the EPR studies. The trapping by H_2 molecules in the lattice has also been recently established by LVM spectroscopy [10,11], and optical detection of EPR [12–14].[5]

The kinetics of the processes have been determined giving for the vacancy migration activation energy, 0.18 ± 0.02 eV in n-type, 0.45 ± 0.04 eV in high-resistivity, and 0.32 ± 0.02 eV in p-type material. These presumably reflect the different properties of the V^{2-}, V^0, and V^{2+} charge states, which are dominant for each of the Fermi level positions in the respective cases.

In addition, as illustrated in Fig. 2, it has been established that the migration and trapping processes can also be made to occur even at 4.2 K under optical excitation, as well as by the ionization accompanying the electron irradiation. The vacancy is therefore a very fragile defect, displaying *athermal* recombination-enhanced motion. At elevated temperatures where diffusion is normally studied, all charge states can exist as the vacancy traps and emits the thermally generated electrons and holes, and each of the above processes will be simultaneously occurring to various degrees. In detail therefore the vacancy migration process is very complicated, but in practical terms, it has the simple result that the contribution of its migration barrier to the activation energy for high temperature thermally activated diffusion is very small. The principal contribution must come from its *formation* energy.

[5] This identification is a subject of current controversy, see Comment by Stallinga and Bech Nielsen [13] and Reply by Chen et al. [14].

5. Vacancy interactions with other defects

In Fig. 3, we show, in addition to the isolated vacancy, the structures deduced for various trapped vacancies, as well as the electrical levels which have been determined for them. When trapped by substitutional Sn, the large Sn atom moves to a position half-way into the vacancy, producing for the neutral state what can be considered as a Sn atom in the center of a divacancy, as illustrated in (c). Its single- and double-donor states are now in normal positive-U ordering, as shown. Interstitial oxygen is an effective trap, moving into the vacancy, as shown in (d), and bonding strongly to two of the vacancy neighbors. The remaining two dangling bonds form an acceptor level at $E_C - 0.17$ eV. Vacancies trapped by the substitutional group-V atoms P, As or Sb take on the configuration shown in (e), introducing a single acceptor level at $E_C - 0.43$, $E_C - 0.47$, or $E_C - 0.44$ eV, respectively. The structure of the divacancy, the result of pairing by two vacancies during vacancy anneal, is shown in (f). It can take on four charge states in the gap, $(VV)^+$, $(VV)^0$, $(VV)^-$, and $(VV)^{2-}$, depending upon whether there are one, two, three, or four electrons trapped into the well-separated remaining two dangling bonds, with the measured level positions, as indicated.

In the case of the Ge-vacancy pair, the electrical level positions have not been directly measured. However, its dangling bond reconstructions, shown in (g) and (h), reveal an only slightly perturbed vacancy, and its general behavior vs. Fermi level, optical excitation, etc., appears identical to that of the isolated vacancy. The level positions have also not been conclusively identified for vacancies trapped by aluminum or boron. Their structures have, however, been determined, with the aluminum atom as nearest neighbor, (*i*), and the boron atom as next-nearest neighbor, (*j*).

Shown also in Fig. 3 (*l*) and (*k*), are a single-vacancy containing one [15], and two [10–12], hydrogen atoms, respectively, which have also been identified by EPR techniques. Combined with the rich variety of hydrogen local vibrational mode absorption spectra observed in hydrogen-implanted material, it has been possible to detect and identify the signatures of the complete set, VH, VH_2, VH_3, and VH_4 [10]. All except VH_4 will have dangling bonds and should be electrically active. No information concerning their electrical level positions are yet available, but, as suggested by their structures, the electrical properties of $V{\cdot}H_2$ can reasonably be

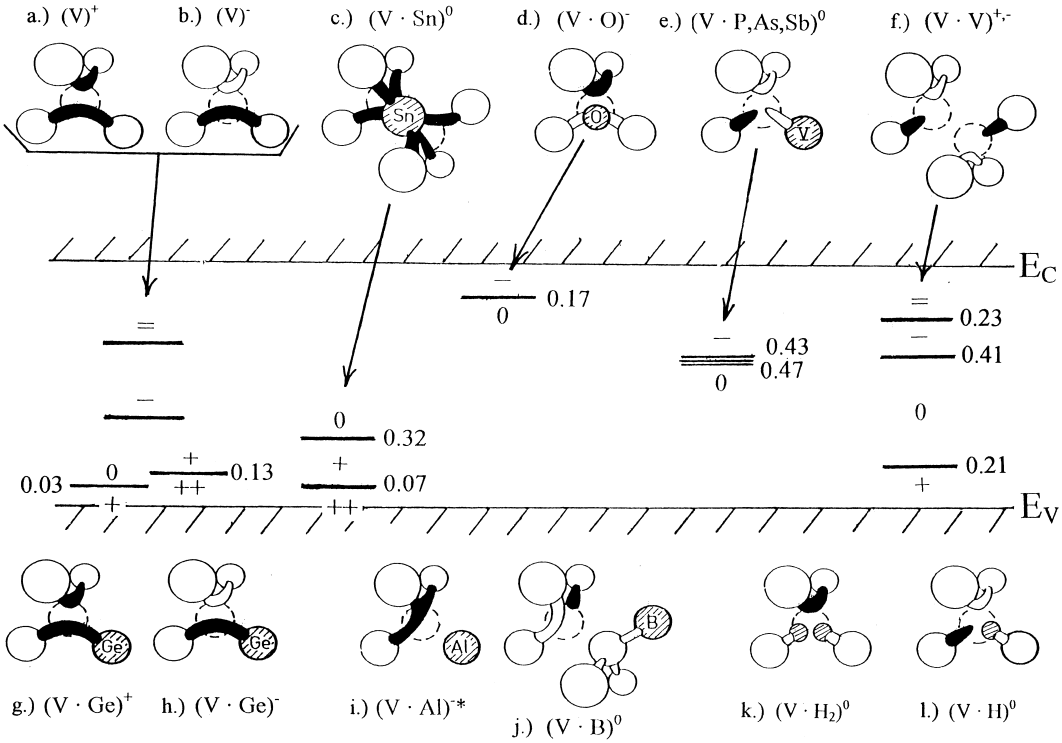

Fig. 3. Structures of trapped vacancies and their electrical level positions (indicated in eV from the nearest band edge), after Ref. [5].

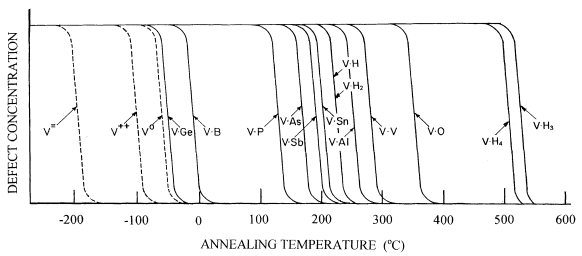

Fig. 4. Schematic of vacancy and vacancy-defect pair annealing stages (~15–30 min isochronal), from Ref. [5].

expected to be similar to that for V·O [12–14] (see footnote 5), and, similarly, V·H to that of V·P [15].

In Fig. 4, the stability of the vacancy and several of the first generation vacancy-defect pairs is summarized schematically, as has been observed in ~15–30 min isochronal annealing studies. The stability of each pair reflects a binding energy between the vacancy and its partner, which, in turn, can produce enhanced vacancy-related diffusion for the partner. Conversely, this vacancy trapping can serve to confuse attempts to extract the true vacancy mobility from conventional diffusion measurements, which attempt to measure the effect of vacancy drift over macroscopic distances.

6. Vacancy aggregates

In heavy particle damage, such as can occur, for example, from protons in the Van Allen belt in space, from neutrons in a nuclear reactor, from the myriad of heavy particles encountered by silicon detectors in high-energy nuclear particle experiments, or in reactive ion etching and ion implant processes, the recoiling atoms have substantial kinetic energy which, in turn, can produce many displacements in a highly localized region. As a result, vacancy aggregation can be expected to dominate over interactions with the more distant isolated impurity dopants. This domain is not as well understood, but an instructive guide can be obtained from EPR studies of neutron-irradiated materials [16–18]. There, identifications of various electrically active small-vacancy aggregates have been proposed and their structures are indicated in Fig. 5. Through the 4-vacancy complex, the {1 1 0} planar structure of the divacancy appears to continue. The addition of a fifth vacancy is believed to be out of the plane. For the di- and tri-vacancies, defects with oxygen tying up the various reconstructed bonds have also been observed suggesting the important stabilizing role of oxygen, as in the single vacancy-oxygen pair of Fig. 3. We can expect these and higher order aggregates to be sources of

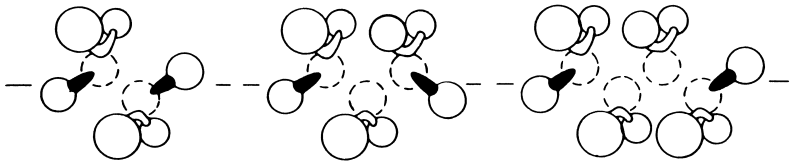

(a) DIVACANCY (b) 3- VACANCY (c) 4-VACANCY

Fig. 5. Structures deduced by EPR of small-vacancy aggregates, with and without oxygen incorporation [16–18].

released vacancies during subsequent elevated temperature processing.

7. The silicon interstitial

In p-type silicon, no EPR evidence of an isolated silicon atom has been observed after in situ electron irradiation at cryogenic temperatures. Instead, only defects which are identified as interstitials trapped at impurities are observed, and in $\sim$1 : 1 concentration to that of the isolated vacancies. From this, it has been concluded that the isolated interstitial atoms must be highly mobile under the electron irradiation conditions in p-type material, even at 4.2 K! This is indicated in Fig. 2, the identified traps being the substitutional acceptors, carbon, molecular hydrogen, and (indirectly) interstitial oxygen. In n-type silicon, defect production is observed to be much lower at cryogenic temperatures, making these experiments much more difficult, but the evidence indicates that migration may not occur until annealing to $\sim$140–175 K, where some of the trapped interstitial configurations are observed to emerge. In either case, however, high mobility for the interstitial is indicated, having executed long-range motion at least by $\sim$175 K, but no direct experimental evidence of its structure or electrical properties is available.

We turn therefore to the trapped interstitials for possible clues as to the structure of the isolated silicon interstitial. In Fig. 6, the structure deduced for the various trapped states is illustrated, along with their corresponding electrical level positions in the band gap. We see a variety of configurations. As trapped by substitutional aluminum, the interstitial silicon has traded places ejecting the Al atom into the high-symmetry tetrahedral interstitial site, as seen in its Al_i^{2+} EPR-active charge state. It is a donor, with its second donor level as indicated. Boron, on the other hand, finds itself displaced into a position slightly off from a bond-centered position between two silicon atoms, as observed in its neutral B_i^0 EPR-active charge state. Its electrical levels have been determined as shown, its acceptor level being substantially lower than its donor level, in negative-U ordering. Carbon ends up in a split-$\langle 1\,0\,0\rangle$ configuration sharing a lattice site with a silicon atom. In this case, all three available charge states retain this configuration, as evidenced by the EPR studies of its positive (C_i^+) and negative (C_i^-) states, and by infrared carbon local vibrational mode studies of the neutral (C_i^0) state [19].

Finally, we include in Fig. 6(d) the configuration for interstitial silicon paired off with two hydrogen atoms, $Si_i{\cdot}H_2$, recently identified from LVM studies [20]. Here, the presence of the two bonding hydrogen atoms causes the silicon split-interstitial configuration to rotate to an orientation intermediate between a $\langle 1\,0\,0\rangle$- and $\langle 1\,1\,0\rangle$-split arrangement, as determined from the symmetry and directions of the various hydrogen stretch vibrations. Although observed in this study after hydrogen implantation, these characteristic LVM bands had previously been observed, but not identified at the time, after electron irradiation of silicon grown in a hydrogen atmosphere [21]. In analogy to $V{\cdot}H_2$, therefore, it can be produced when interstitial silicon is trapped by molecular H_2 in the lattice.

A wide variety of possible configurations are therefore suggested for the isolated interstitial from these interstitial-related defects. Let us therefore now turn to modern state-of-the-art theory to see what it may be able to contribute. First, as a test, let's consider how well they do for the trapped interstitials. In the case of $Si_i{\cdot}H_2$, the recent experimentally determined configuration is found to agree in remarkable detail with theoretical predictions [20,22]. Similarly, recent theoretical calculations have confirmed the experimentally observed configurations for interstitial carbon [23,24,]. In the case of interstitial boron, a configuration similar to that observed by EPR was predicted for the neutral state, and also for the negative one [25]. However, the lowest-energy configuration for the positive charge state was predicted to occur as the boron atom reassumes its substitutional position ejecting the silicon atom back into the nearby tetrahedral interstitial site. These predicted configurational changes fit in quite nicely with several otherwise difficult to explain EPR observations, and are currently believed therefore to be essentially correct. They also provide a possible mechanism for the

negative-U ordering experimentally observed for its levels, as shown in Fig. 6.

Encouraged by the above apparent successes, we now consider the theoretical results for the isolated silicon interstitial. In Fig. 7, we present the predicted total energy diagram for various configurations of Si_i^0 and its two ionized states, $Si_i^+ + e^-$ and $Si_i^{2+} + 2e^-$, where we have combined the results of two research groups [26,27]. Like the results mentioned above for trapped interstitials, these results were also obtained from ab-initio total energy calculations involving the local density approximation and are therefore presumably representative of the best current state-of-the-art capabilities. We note first that the predicted stable configurations are different for the three charge states: Si_i^0 in a $\langle 1\,1\,0\rangle$ split "X" configuration, Si_i^+ in the bond-centered "B" configuration, and Si_i^{2+} in the high-symmetry "T" tetrahedral position. Further, since each of these configurations represent saddle points for migration between any of the others, the indicated energies can provide estimates of the activation energy for migration in each charge state. We note that the predicted barrier is particularly small in the Si_i^+ charge state, perhaps providing already an explanation of the high observed mobility of the interstitial. But in addition, we are led immediately to another mechanism, when we recognize that these results imply that simply changing its charge state by capture of a carrier invariably brings it to a

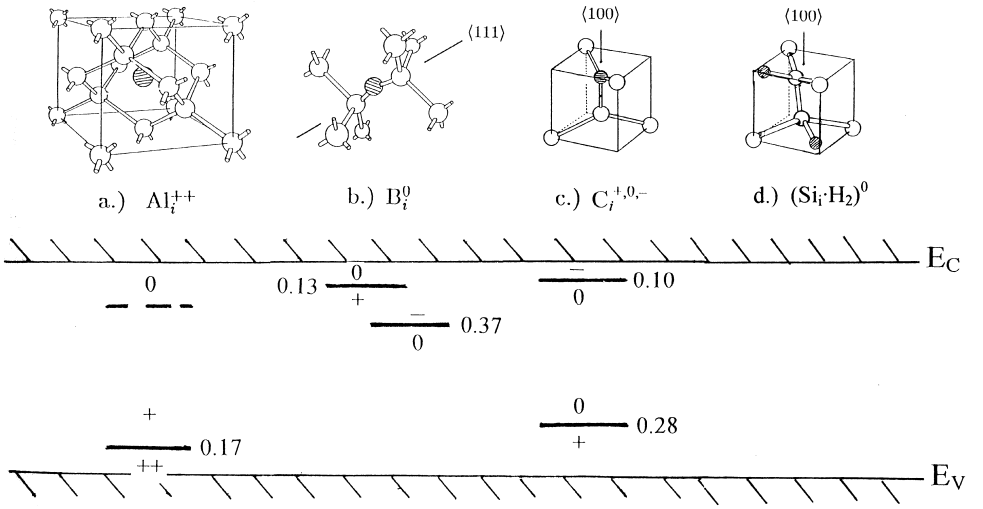

Fig. 6. Trapped interstitials, and their level positions (eV from the closest band edge), from Ref. [5].

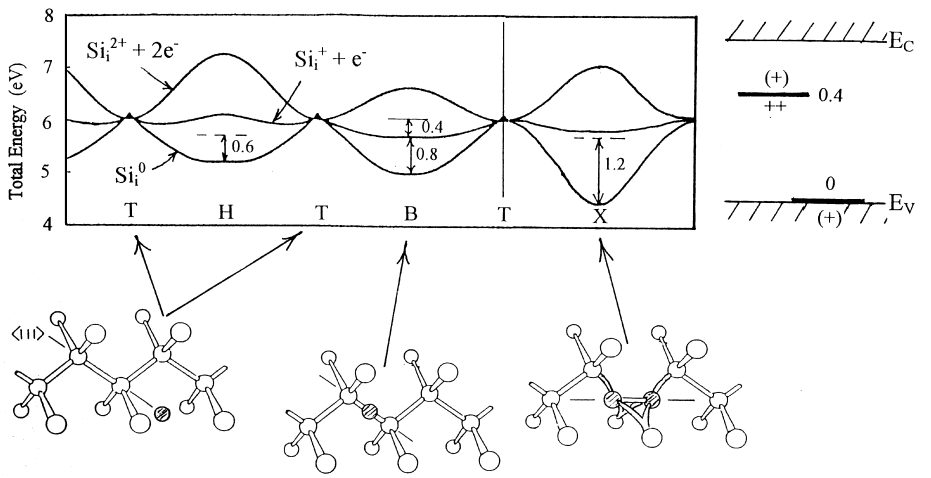

Fig. 7. Total energy diagram vs lattice configuration as predicted by theory [26,27] for three charge states of interstitial silicon. The implied level positions are illustrated on the right. From Ref. [4].

saddle point configuration from which further carrier capture or release allows migration. Recognizing that there is significant ionization produced during electron irradiation, this athermal recombination-enhanced process provides a logical explanation for the high mobility observed in the p-type studies.

Also implied in the curves is the remarkable level position ordering indicated to the right of the figure. The true electrical level position of a defect is defined as the energy difference between the *relaxed* ionized and unionized states. The first donor level $(0/+)$ position below the conduction band edge is therefore given by the energy difference between Si_i^0 in its lowest energy X configuration and $Si_i^+ + e^-$ in its lowest energy B configuration, predicting $E_C - 1.2\,eV$, i.e., right at the valence band edge! The second donor level is given, in turn, by the energy difference between the B configuration of $Si_i^+ + e^-$ and the T position of $Si_i^{2+} + 2e^-$, giving $E_C - 0.4\,eV$. A very large negative-U ordering is therefore predicted, perhaps explaining why the paramagnetic Si_i^+ charge state has not revealed itself even in n-type material, where the interstitial appears to be stable at least up to ~140 K. In such a negative-U situation, the intermediate Si_i^+ EPR-active charge state is thermodynamically unstable, and with the neutral state so deep it may be difficult to optically excite it, as was possible in the vacancy and interstitial boron negative-U cases.

In spite of the fact therefore that the isolated interstitial silicon atom has not been directly observed, we have reason to feel we may understand it pretty well. Like the vacancy, the evidence is that it diffuses easily through the lattice, having migrated large distances in n-type silicon by ~140 K, and, under the electron irradiation conditions in p-type, very efficiently, even at 4.2 K.

8. Interstitial-related reactions

In Fig. 8, we illustrate schematically the dominant EPR- and LVM-identified annealing reactions associated with the interstitial-related defects, as would be observed in a typical 15–30 min isochronal annealing sequence. When interstitial carbon disappears at ~50°C, new defects emerge which have been identified directly by EPR to be interstitial carbon paired with substitutional carbon, interstitial oxygen, and substitutional group-V donors, revealing unambiguously that the annealing stage is the result of long-range diffusion of the carbon. Kinetic studies of the process give for the interstitial carbon diffusion activation energy, 0.80–0.87 eV.[6] The disappearance of interstitial aluminum at

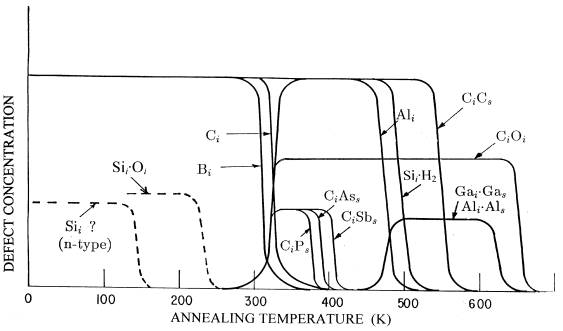

Fig. 8. Schematic of interstitial-related defect annealing stages (~15–30 min isochronal).

~225°C is accompanied by the emergence of a defect identified as Al_i-Al_s, revealing its long-range migration at this temperature to be trapped by substitutional aluminum. Its activation energy for diffusion has been measured to be 1.2 eV. The emergence of Ga_i-Ga_s pairs in the same temperature region in Ga-doped silicon, reveals the similar formation of interstitial Ga by the irradiation and its subsequent migration to form pairs.

Interstitial boron disappears at ~−35–+25°C, depending upon its charge state, the kinetics studied by both EPR and DLTS revealing an activation energy in either case of 0.6 eV. No new EPR-active defects have been observed to emerge, however, to establish unambiguously its fate. On the other hand, systematic DLTS studies have provided strong evidence for its long-range migration to form pairs with interstitial oxygen, and substitutional carbon and boron [29]. The 0.6 eV activation energy is therefore that for isolated interstitial boron diffusion.

In all of these cases, therefore, the silicon interstitial that has been trapped by an impurity has a limited stability, but, at a suitable temperature migrates as an entity, i.e., as the corresponding displaced interstitial impurity until it is further trapped by other impurities. To each it has a certain binding energy, and as the temperature is raised it is released from those centers to which the binding is weak, and retrapped to form the more stable complexes, etc. This trap-limited process has been confirmed in quantitative detail by DLTS studies [29]. Also shown in the figure is a weak trapping of interstitial silicon by interstitial oxygen which has been inferred by DLTS from an increase at ~−50°C of interstitial carbon and interstitial boron, which occurs only in oxygen-containing Czochralski-grown material.

Finally, both B_i and Al_i display strong recombination-enhancement in their diffusion. For B_i, its annealing can be made to occur athermally at cryogenic temperatures under optical or electrical injection conditions [9], as might be expected from the large configurational changes vs. charge state predicted by theory. For Al_i, the 1.2 eV barrier for thermally activated diffusion is

[6] A recent excellent review of the role of carbon in silicon, which combines information obtained from EPR, DLTS, and optical studies, is given by Davies and Newman [28].

reduced to ~0.3 eV under injection conditions, leading to the proposal that for its neutral state it too probably distorts strongly as its outer valence shell picks up a p-electron which prefers a bonding arrangement [9,30,31].

9. Interstitial aggregates

Again, in heavy particle displacement damage, we can expect aggregation of interstitials to occur and dominate over their individual interactions with isolated impurities. EPR studies in neutron-irradiated silicon have found two distinct but very similar defects, each of which has been suggested by the respective authors to arise from a silicon di-interstitial [32,33]. Apart from this, there is no further EPR information. However, one should mention the "{3 1 1}" defects detected in high-resolution lattice-imaged TEM after ion implant processing. The 1 : 1 correlation between their elevated temperature disappearance and simultaneously occurring enhanced impurity diffusion processes identified with interstitials provides a very strong argument to identify them with planar aggregates of interstitials formed as a result of the ion implantation [34,35].[7]

10. Close Frenkel pairs

In the interpretation of the above results, it has been commonly assumed that competition between annihilation and separation of the close vacancy-interstitial (Frenkel) pairs is occurring during a low-temperature irradiation, and that only the separated pairs survive [1–3]. However, using X-ray diffuse scattering techniques, Erhart and Zillgen have concluded very recently that, instead, the escaped vacancies and interstitials comprise only a fraction of the pairs produced. They conclude that close Frenkel pairs, presumably electrically inactive, remain, annealing out only slowly in the range up to room temperature [36]. This is a very interesting new result, and, *if correct*, must force a reconsideration of the basic processes occurring during the primary damage event. It should have no effect, however, upon the understanding that we have obtained concerning the escaped isolated interstitials and vacancies and their subsequent migration and interactions with other defects.

11. Summary

Both the isolated vacancy and interstitial are highly mobile, diffusing macroscopic distances until trapped by impurities or other defects at temperatures well below room temperature. Their activation energies for migration are therefore very low, and the activation energy for the contribution of each to thermally activated bulk self- and impurity diffusion must come primarily therefore from the *formation* energy of each. This fact has been difficult to swallow in the diffusion community over the many years since the first in the series of EPR results on the vacancy (1962) and the interstitial (1964) were published. It is interesting to note, however, that these low vacancy and interstitial activation energies for migration are beginning to show up more and more in the analysis of diffusion in the recent literature, and are beginning to be accepted. In some cases, theory is also coming up with the same conclusions [37]. It is becoming more and more clear that the higher activation energies deduced earlier were probably reflecting the *trap-limited* migration of the intrinsic defects. A glance at Figs. 4 and 8 provides all of the evidence needed to justify this conclusion.

In the annealing after reactive ion etch or ion-implant processing, transient release of vacancies and interstitials can be expected. The rich hierarchy of reactions that we have described here for single vacancies and interstitials vs annealing can be a useful guide for what to expect in these cases as well. It is clear that the interstitial is the most dangerous culprit because when trapped by acceptors or carbon, the resulting complex is highly stable and diffuses rapidly as an entity, with a thermal activation barrier for B_i of only 0.6 eV, for C_i, only 0.80–0.86 eV. And, for B_i, the diffusion can be further enhanced strongly under ionization conditions. They are, in turn, trapped by other impurities, but only to be re-released at higher temperatures. In effect, the interstitial B_i and C_i continue to diffuse as entities in a trap-limited mode. Therefore long-range redistribution of these impurities can be expected, as observed in the transient-enhanced diffusion of boron after ion implantation.[8] Also, we note the competition between boron and carbon as traps for the interstitials. This serves to help explain also the reduction experimentally observed in the transient-enhanced diffusion of boron in device structures containing a high carbon content [38].

Our observations for the vacancy reactions suggest that it should play a somewhat less important role in transient-enhanced processes. This is because interchange between the impurity and its bound vacancy does not by itself serve to move the impurity. It can only occur if the vacancy separates from the impurity by two single jumps to the third nearest-neighbor separation and then returns to a different neighbor position, followed by vacancy–impurity interchange. This means that it is only the much weaker binding energy

[7] See also the several articles on this topic in [35].

[8] See, for example, the several articles on this topic in [35].

remaining at the third neighbor site that holds the two together during each diffusional jump as an entity, and separation of the two occurs easily, discouraging long-range migration of the complex as an entity, particularly as the temperature is raised.

Acknowledgements

The early EPR work described here was performed by me while at the General Electric Research Laboratory from 1960–1975. Most of the remaining work has been performed by my students at Lehigh University under the continued support of the Office of Naval Research over the period 1976–1993.

References

[1] Watkins GD. In: Schröter W, editor. Electronic structure and properties of semiconductors [Chapter 3]. In: Cahn RW, Haasen P, Kramer EJ, editors. Materials science and technology, vol. 4. Wheinheim: VCH, 1991.
[2] Watkins GD. In: Jackson KA, Schröter W, editors. Handbook of semiconductor technology, vol. 1. Weihneim: Wiley-VCH, 2000 [Chapter 3].
[3] Watkins GD. In: Pantelides ST, editor. Deep centers in semiconductors. New York: Gordon and Breach, 1986 [Chapter 3].
[4] Watkins GD. In: Diaz de la Rubia T, Stolk PA, Rafferty CS, editors. Defects and diffusion in silicon processing. MRS Symposium, vol. 469, Warrendale, 1997. p. 139.
[5] Watkins GD. In: Hull R, editor. Properties of crystalline silicon. London: INSPEC, 1999 [Chapter 11.1].
[6] Watkins GD. In: Grosse P, editor. Festkörperprobleme (Advances in Solid State Physics), vol. XXIV. Braunschweig: Viewig, 1984. p. 163.
[7] Kimerling LC. Sol St Electr 1978;21:1391.
[8] Bourgoin JC, Corbett JW. Rad Effects 1978;36:167.
[9] Watkins GD, Chatterjee AP, Harris RD, Troxell JR. Semic and Ins 1983;5:321.
[10] Bech Nielsen B, Hoffmann L, Budde M, Jones R, Goss J, Ödberg S. Mater Sci Forum 1995;196–201:933.
[11] Bai GR, Zhou JK, Chen JM, Shi TS, Qi MW, Xie LM. Sci Sinica A 1988;31:499.
[12] Chen WM, Awaldekarim OO, Monemar B, Lindström JL, Oehrlein GS. Phys Rev Lett 1990;64:3042.
[13] Stallinga P, Bech Nielsen B. Phys Rev Lett 1998;80:422.
[14] Chen WM, Awaldekarim OO, Monemar B, Lindström JL, Oehrlein GS. Phys Rev Lett 1998;80:423.
[15] Bech Nielsen B, Johannesen P, Stallinga P, Bonde Nielsen K. Phys Rev Lett 1997;79:1507.
[16] Brower KL. In: Corbett J, Watkins GD, editors. Radiation effects in semiconductors. New York: Gordon and Breach, 1971. p. 189.
[17] Lee Y-H, Corbett JW. Phys Rev B 1974;9:4351.
[18] Lee Y-H, Corbett JW. Phys Rev B 1973;8:2810.
[19] Zheng JF, Stavola M, Watkins GD. In: Lockwood DJ, editor. 22nd International Conference on the Physics of Semiconductors. Singapore: World Scientific, 1995. p. 2363.
[20] Budde M, Bech Nielsen B, Leary P, Goss J, Jones R, Briddon PR, Öberg S, Breuer SJ. Phys Rev B 1998; 57:4397.
[21] Shi TS, Bai GR, Qi MW, Zhou JK. Mater Res Forum 1986;10–12:597.
[22] Van de Walle CG, Neugebauer J. Phys Rev B 1995;52: R14320.
[23] Capaz RB, Dal Pino Jr A, Joannopoulos JD. Phys Rev B 1994;50:7439.
[24] Leary P, Jones R, Örberg S, Torres VJB. Phys Rev B 1997;55:2188.
[25] Tarnow E. Europhys Lett 1991;16:449.
[26] Car R, Kelly PJ, Oshiyama A, Pantelides ST. In: Kimerling LC, Parsey Jr JM, editors. Thirteenth International Conference on Defects in Semiconductors. Warrendale: Metallurgical Soc. of AIME, 1985. p. 269.
[27] Bar-Yam Y, Joannopoulos JD. In: Kimerling LC, Parsey Jr JM, editors. Thirteenth International Conference on Defects in Semiconductors. Warrendale: Metallurgical Soc. of AIME, 1985. p. 261.
[28] Davies G, Newman RC. In: Mahajan S, editor. Handbook on semiconductors, vol. 3. Amsterdam: Elsevier Science B.V, 1994. p. 1557.
[29] Kimerling LC, Asom MT, Benton JL, Devrinski PJ, Caefer CE. Mater Sci Forum 1989;24–41:141.
[30] Troxell JR, Chatterjee AP, Watkins GD, Kimerling LC. Phys Rev B 1979;19:5336.
[31] Baraff GA, Schluter M, Allan G. Phys Rev Lett 1983;50:739.
[32] Brower KL. Phys Rev B 1976;14:872.
[33] Lee Y-H, Gerasimenko NN, Corbett JW. Phys Rev B 1976;14:4506.
[34] Eaglesham DA, Stolk PA, Gossmann H-J, Poate JM. Appl Phys Lett 1994;65:2305.
[35] Diaz de la Rubia T, Coffa S, Stolk PA, Rafferty CS, editors. Defects and diffusion in silicon processing. MRS Symposium, vol. 469, Warrendale, 1997.
[36] Erhart P, Zillgen H. In: Diaz de la Rubia T, Coffa S, Stolk PA, Rafferty CS, editors. Defects and diffusion in silicon processing. MRS Symposium, vol. 469, Warrendale, 1997. p. 175.
[37] Blöchl PE, Smargiassi E, Car R, Laks DB, Asdreoni W, Pantelides ST. Phys Rev Lett 1993;70:2435.
[38] Eaglesham DJ, Stolk PA, Gossmann H-J, Haynes TE, Poate JM. Nucl Instr and Meth B 1995;106:191.